Research Article | Vol. 29, No. 11 / 24 May 2021 / Optics Express 16506
Optics EXPRESS

Active tapered double-clad fiber with low birefringence

ANDREI FEDOTOV,[1,*] VASILII USTIMCHIK,[2] JOONA RISSANEN,[3] ALEXANDER KOLOSOVSKII,[4] VICTOR VOLOSHIN,[4] IGOR VOROB'EV,[4] REGINA GUMENYUK,[1] YURI CHAMOROVSKIY,[4] AND VALERY FILIPPOV[3]

[1]*Tampere University, Kalevantie, 33100 Tampere, Finland*
[2]*Peter the Great St. Petersburg Polytechnic University, Polytechnicheskaya str. 29, 195251 St. Petersburg, Russia*
[3]*Ampliconyx Ltd, Lautakatonkatu 18, 33580 Tampere, Finland*
[4]*Kotel'nikov Institute of Radio Engineering and Electronics (Fryazino Branch) Russian Academy of Science, Vvedenskogo Sq. 1, 141190 Fryazino, Russia*
[*]*andrei.fedotov@tuni.fi*

Abstract: We addressed the problem of a state of polarization (SOP) drift caused by heating under intense clad pumping in different types of active tapered double-clad fibers. We investigated experimentally the variations of the SOP and degree of polarization (DOP) under clad pumping in polarization-maintaining (PANDA type) and regular (non-PM) Yb-doped double-clad large mode area tapered fibers. We discovered that the birefringence of active fibers is highly dependent on the launched pump power. To solve the problem of the SOP drift in active large mode are fibers, we, for the first time to the best of our knowledge, presented an active double-clad fiber with low intrinsic birefringence as a gain medium. An Yb-doped spun tapered double-clad fiber (sT-DCF) with intrinsic birefringence as low as 1.45×10^{-8} was manufactured and experimentally studied. We have proved experimentally that the DOP and SOP remains more stable in sT-DCF with increasing pump power compared to PM PANDA-type and regular non-PM tapered double-clad fibers. In particular, the SOP drift in sT-DCF is almost one order of magnitude less than in other tapered fibers, while the DOP drift in sT-DCF is comparable with the drift in PANDA-type fiber and one order of magnitude less than in the non-PM tapered fiber. An active sT-DCF showing efficient amplification was demonstrated in an all-fiber-based picosecond master-oscillator power-amplifier scheme. The system delivered 50 ps pulses at 1040 nm with an average power of 50 W, 34 dB gain, 26 μm MFD and perfect beam quality.

1. Introduction

The technology of fiber lasers and amplifiers has been developed extremely rapidly over the past two decades. One of the most important components of such devices is an active optical fiber doped with rare-earth elements (Er, Yb, Tm, Nd, Pr, etc.). Undesirable non-linear effects are one of the main factors limiting its performance. To increase the threshold of the nonlinear effects, it is necessary to use a fiber with a large mode area (LMA). It is important that the enlarged fiber core only supports the propagation of the fundamental mode and preserves a stable state of polarization (SOP). The stability of the SOP is critically important for a number of applications such as nonlinear light frequency conversion or coherent beam combining.

There are three main types of active large mode area fibers described in the literature that are able to maintain a state of polarization: active polarization-maintaining (PM) LMA fibers with a low numerical aperture (NA) [1], micro-structured active polarization-maintaining fibers [2], and active PM tapered double-clad fibers (T-DCF) [3]. To maintain a stable SOP the common approach in optical fibers is to utilize the concept of creating strong internal mechanical

#421958 https://doi.org/10.1364/OE.421958
Journal © 2021 Received 4 Feb 2021; revised 27 Apr 2021; accepted 28 Apr 2021; published 13 May 2021

Optics EXPRESS

stress frozen inside the fiber by adding glass elements with significantly different thermal expansion coefficients (PANDA, bow-tie, or stress clad) to the preform. This SOP stabilization method was originally developed in the 1980s for passive optical fibers intended to be used in telecommunication and sensor systems [4–6]. A common drawback of such birefringent fibers is the significant temperature sensitivity. Internal birefringence sharply changes with temperature [4,5]. Furthermore, these changes occur irreversibly forming hysteresis [4]. During annealing, both an increase and a decrease in the internal birefringence are possible. Since changes in birefringence form hysteresis, fibers with strong birefringence have a memory of the heating [4–7]. However, due to the nature of the application (as optical waveguide), highly birefringent passive fibers rarely undergo significant temperature changes, and none of the aforementioned drawbacks usually limit their use [7].

With the advent of active optical fibers, this approach (strong internal mechanical stress) was automatically applied to them to achieve stable output polarization. It should be noted that the conditions of exploiting active and passive fibers are fundamentally different. Passive fibers are usually long, and they are subjected to mechanical stresses, for example compression, stretching and mechanical vibrations. Unlike passive optical fibers, active fibers in lasers/amplifiers are usually relatively short (no more than 20-30 m), always well isolated from mechanical actions by a device casing and, most importantly, they always heat up internally during operation. The internal heating of the active fiber caused by pumping has been well studied in the literature [8–12]. Recently, Lou et al. [12] showed experimentally that the temperature of the core of a clad-pumped active fiber varies greatly (by several degrees Celsius) in the longitudinal direction, with a typical spatial period of several centimeters. This causes a change in internal stress, which in turn leads to a variation of the local eigenstates of the fiber, and, as a result, changes of the SOP, polarization extinction ratio (PER), and even the degree of polarization (DOP) during operation.

In this paper, we address the problem of DOP and SOP changes in active LMA double-clad tapered fibers caused by heating under clad pumping. We experimentally evaluated the dependence of polarization on pumping in active non-PM and PANDA type T-DCF. To preserve the DOP and SOP in the active LMA fiber, our solution is an Yb-doped spun T-DCF with low internal birefringence ($\sim 10^{-8}$). This is demonstrated for the first time to the best of our knowledge. Low birefringence (Lo-Bi) was achieved by rotating the preform at a constant speed during fiber drawing. We investigated the polarization and amplification properties of the manufactured Lo-Bi active spun tapered fiber (sT-DCF). An all-fiber picosecond MOPA system based on the sT-DCF provided an efficient direct amplification (34 dB gain) of a 50 ps pulse signal to 50 W with excellent beam quality.

2. Drift of the polarization state in active fibers caused by clad pumping

In any application requiring the use of polarized light, it is extremely important to maintain high stability of the polarization parameters over the entire operating range. The absolute value of retardance in an optical medium (i.e., phase shift between the “slow" and “fast" polarization modes) fundamentally determines the output SOP. Optical fiber is no exception and retardance there can be described by the formula:

$$R = 2\pi\Delta nL/\lambda = \beta L, \tag{1}$$

where Δn is the difference in the refractive index for “slow" and “fast" polarization modes and represents normalized birefringence $B = n_s - n_f = \beta \cdot \lambda/2\pi$, λ is the wavelength of light propagating in a fiber, L is fiber length, $\beta = 2\pi\Delta n/\lambda$ is birefringence of a fiber and is taken to be constant along the light propagation length. Equation 1 describes birefringence as a non-local parameter of the entire fiber. However, in general, birefringence may slightly change along the fiber length under external and internal perturbations. In cases when both polarization eigenstates

Optics EXPRESS

are excited, the temperature sensitivity of the retardance is defined by the equation:

$$dR = \left(L\frac{d\beta}{dT} + \beta\frac{dL}{dT}\right)\Delta T, \tag{2}$$

where L ~1-10 m, B ~10^{-4} [3], $(1/L)\cdot dL/dT = 5\cdot 10^{-7}/^{\circ}$C, $d\beta/dT = 10^{-5}$rad/m $\cdot^{\circ}$ C [13]. It can be stated that the output SOP of light transmitted through any birefringent medium depends on the absolute value of retardation only if the input SOP of the light does not precisely coincide with the polarization eigenstate of the medium. Even with an exact coincidence of the input SOP and the polarization eigenstate of the fiber, the output SOP can be disturbed by the micro inhomogeneities of real optical fiber samples. However, the light coupling is quite far from the ideal case and the PER of the input light has a finite value. So, it can be declared that both eigen polarization modes are always excited in the real fiber samples. Therefore, as seen from Eq. (2), the temperature sensitivity of SOP is determined by the fiber length L, the absolute value of birefringence β, the temperature sensitivity of birefringence $d\beta/dT$, and the fiber length dL/dT. Thus, the SOP of the propagating light is more sensitive to temperature changes, the higher the intrinsic birefringence of the fiber and the longer the fiber itself. For the relatively short fiber lengths that are usually exploited in lasers/amplifiers, the first term in Eq. (2) is five orders of magnitude larger than the second one. So, Eq. (2) can be simplified:

$$dR = L\frac{d\beta}{dT}\Delta T \tag{3}$$

The temperature sensitivity of the retardance is determined by the fiber length L and by the temperature sensitivity of birefringence $d\beta/dT$ [Eq. (3)]. Therefore, the SOP (azimuth ϕ and ellipticity θ), in turn, is a function of retardance [14]:

$$\phi = \frac{\cos R}{1-|\chi^2|},\ \theta = \frac{\sin R}{1+|\chi^2|}, \tag{4}$$

where $\chi = A_y/A_x e^{iR}$ is a complex parameter of SOP, and A_x and A_y are amplitudes of electrical vector. As follows from Eq. (4), azimuth and ellipticity are in quadrature with respect to the retardance. The pump radiation launched into the cladding heats the fiber internally and thereby changes the retardance as a result of the temperature sensitivity of the birefringence [Eq. (3)]. The retardance variations are reflected in the change of SOP [Eq. (4)].

Since the passive fibers undergo low-temperature variations, the sensitivity of the SOP of the propagating light is negligible. However, for active fibers the core temperature rises dramatically under substantial pumping, this being especially pronounced for a high-power fiber laser system based on LMA fibers [12]. This means the SOP changes with pumping, which negatively affects the output polarization performance.

In this paper, we investigated the dependence of DOP and SOP as a function of clad pumping for three different types of active tapered fibers: regular (non-PM) T-DCF, highly birefringent PANDA-type T-DCF and low birefringent spun T-DCF. All of them were manufactured by SPCVD technology. The parameters of the studied tapered fibers are presented in Supplement 1 (Table S1).

2.1. Polarization drift caused by clad pumping in an active non-PM T-DCF

We have experimentally investigated the polarization properties of a non-PM active tapered fiber, whose longitudinal profile and end face picture are shown in Fig. 1(a). The total length of the non-PM T-DCF was 3.2 m. The numerical aperture (NA) of the first clad and the core were 0.46 and 0.1, respectively. An ytterbium double-clad non-PM tapered fiber had a core-to-cladding diameter ratio of 1:8 with an output core diameter of 100 μm. The only fundamental mode was excited in the narrow end of the tapered fiber.

Optics EXPRESS

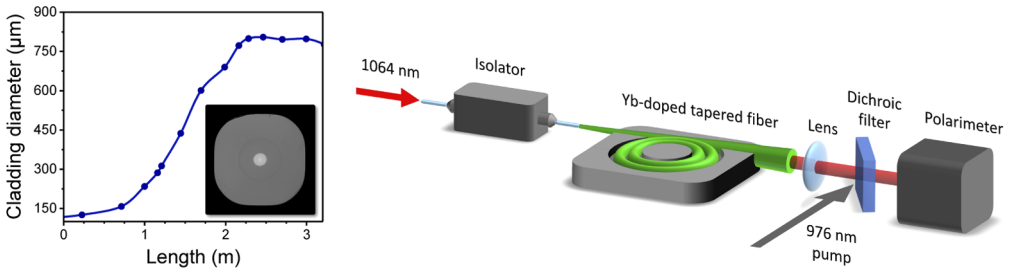

(a) (b)

Fig. 1. (a) Longitudinal profile and end face image (inset) of the non-PM T-DCF, and (b) experimental setup.

The evolution of the output polarization caused by the clad pumping in active tapered fibers was investigated during amplification of a pulsed laser signal on the experimental setup presented in Fig. 1(b). The evaluation process was conducted in the active mode when a seed signal was amplified in an active T-DCF using a clad pumping scheme. As a seed source, we used a commercially available 1064 nm gain-switched laser diode that generated 95 ps pulses at 100 MHz with an ultra-narrow linewidth of 20 pm and average power of 1.5 mW. The ultra-narrow linewidth of the seed source ensured high accuracy of the polarization measurements. The low-power seed signal was pre-amplified up to 20 mW of average power. The polarization-sensitive isolator was used to ensure unidirectional light propagation between the low-power and high-power amplifier cascades. The input PER determined by the isolator parameters was 29.3 dB. The active T-DCF was pumped by a 976 nm multimode laser diode through the dichroic filter to the wide side of the T-DCF. The maximum power was limited to 23 W to eliminate the possibility of polymer degradation or damage. The active tapered fiber was coiled into a 35 cm diameter ring. We did not take any measures for cooling of the T-DCFs during the experiment, since our goal was to identify the dependence of the change in the SOP on the pump-induced heating. The amplified signal with output power of 2.3 W was collimated and then analyzed by a commercial polarimeter.

The output SOP was characterized by measuring the azimuth, ellipticity, and degree of polarization (DOP) of the amplified radiation as a function of the launched pump power and fiber temperature (Fig. 2). PER was calculated from the ellipticity as $10\log_{10}(\tan[\text{ellipticity}])$.

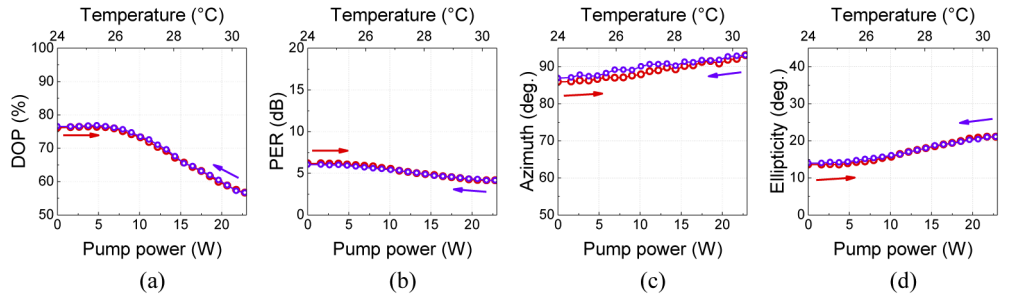

(a) (b) (c) (d)

Fig. 2. (a) DOP, (b) PER, (c) azimuth, and (d) ellipticity vs pump power and fiber temperature for a non-PM T-DCF.

In addition, we also measured the temperature of the active tapered fiber at a distance of 5 cm from the wide end using a thermocouple. The temperature of the cladding reached 30°C at maximum pump power. As follows from the measurement results, a non-PM active tapered fiber

Optics EXPRESS

significantly depolarizes the light propagating and being amplified in it. Moreover, the degree of polarization significantly degraded by 20.2% with increasing pump power from 0 to 23 W.

2.2. Polarization drift caused by clad pumping in an active PANDA-type T-DCF

The polarization sensitivity of an active PANDA-type T-DCF has been verified experimentally by using the same optical scheme as described before [Fig. 1(b)]. The active PANDA-type tapered fiber was 2.2 m long and had 40 μm core with 32 μm MFD (Fig. 3). The PER was 15 dB in a passive regime. A linearly polarized light at 1064 nm was launched into it along the slow axis so that only one polarization mode (one polarization eigenstate) was excited. As in the previous experiment, we measured the dependence of azimuth, ellipticity, and degree of polarization of the output radiation as a function of the launched pump power. The results are shown in Fig. 4.

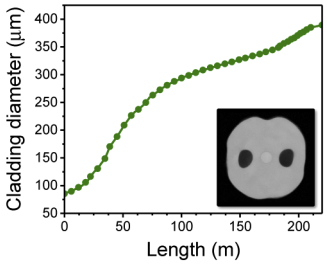

Fig. 3. Longitudinal profile and end face image (inset) of an active PANDA-type T-DCF.

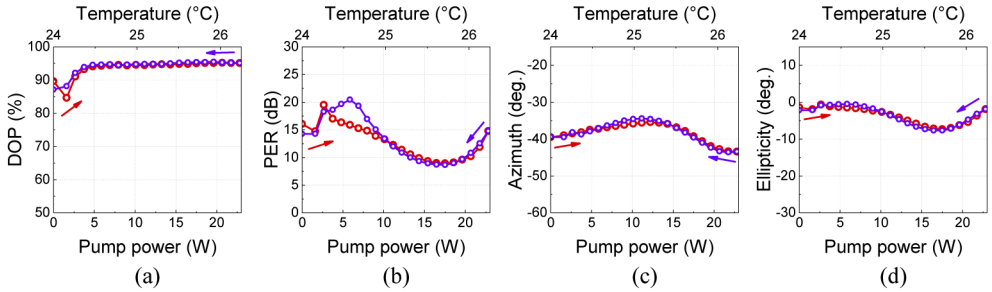

Fig. 4. (a) DOP, (b) PER, (c) azimuth, and (d) ellipticity vs pump power and fiber temperature for an active PANDA-type T-DCF.

The degree of polarization started from 87% because some of the signal leaked to the cladding when the narrow end of the tapered fiber with an 8 μm core was spliced with the 10 μm single-mode fiber. When the tapered fiber was pumped, the signal in the cladding remained the same, while the signal from the core was amplified, so the DOP rose to 94%. The experimental results show that the increase of pump power up to 23 W leads to an increase of the fiber temperature by 2°C (from 24°C at 0 W up to 26°C at 23 W), resulting in periodical changes of the azimuth of the SOP with an amplitude of 8.9° (Fig. 4). At the same time, the change of ellipticity was 7.2° (Fig. 4). The polarization extinction ratio as a function of launched pump power shown in Fig. 4 changed by 11.5 dB when the temperature of the fiber only changed by 2°C. Slight hysteresis was caused by the inertia of heating and cooling. Based on the experimental results, we can draw the following conclusions: (a) the change in the degree of polarization insignificant, being only 1% in the pumping range 5-23 W [Fig. 4(b)]; (b) in an active fiber with a strong birefringence, the PER and SOP (azimuth and ellipticity) of amplified light depend significantly on the launched pump power level.

Optics EXPRESS

2.3. Polarization drift caused by clad pumping in an active T-DCF with low birefringence

The literature describes several basic technologies to produce fibers with low birefringence. One approach is to "idealize" the fiber by making it extremely symmetrical, with a minimum level of internal stress [15]. These objectives were achieved by paying careful attention to the fabrication process. Compensated fibers are an alternative approach to the “ideal" fiber. In this approach, a very low level of internal birefringence can be achieved by choosing doped fiber materials so that the birefringence of the stresses B_s together with the birefringence of the geometric shape of Bc add up to zero [16]. A third class of fibers is produced by the rapid rotation of the preform during the drawing process. This produces so-called spun fibers with low internal birefringence (Lo-Bi fiber) [17]. During rotation of the preform, the fast and slow birefringence axes along the fiber periodically interchange, which leads to partial compensation of the relative phase delay between the eigenpolarization modes [18]. There is a certain averaging that causes symmetrization of the core, which ultimately leads to a significant decrease in the internal birefringence. We have used this last approach to manufacture a spun Yb-doped tapered double-clad fiber (sT-DCF).

2.3.1. Manufacture of an active sT-DCF

The sT-DCF was manufactured using a similar technology to that which was previously used for a passive spun fiber [19]. The step-index Yb-doped preform was assembled with a core-to-cladding diameter ratio of 1:8 [Fig. 5(a)]. The in-core absorption was 700 dB/m at 976 nm, and the core numerical aperture was 0.1. To improve absorption in the sT-DCF, the first cladding was shaped into a square with rounded corners [Fig. 5(b), inset].

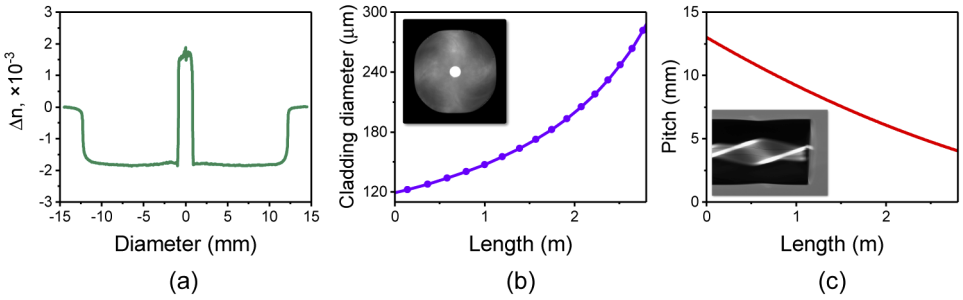

Fig. 5. (a) refractive index profile of the preform; (b) outer cladding diameter vs length of sT-DCF. Inset: the end face image of the fiber; (c) The pitch as a function of the cladding diameter. Inset: the side view of the sT-DCF.

During the drawing process, the fiber rotated at a constant angular velocity of 600 rev/min, while the drawing speed continuously changed to form the fiber into a conical shape. Previously, we have demonstrated that in an sT-DCF with a core of 100 μm and a pitch of 2 mm, the output beam is not Gaussian [20]. Therefore, we cut the sT-DCF step by step from the wide side as far as the 35/280 μm core/cladding, at which point we reached a purely single-mode regime, which was confirmed by the M^2 measurement. Thus, the core/cladding diameter varied from 35/280 μm to 15/125 μm along the 2.75 m length. The longitudinal profile of the sT-DCF is shown in Fig. 5(b). Since the rotating speed was kept constant while the drawing speed varied, the pitch of the sT-DCF also varied along the length of the fiber from 13 mm down to 4 mm towards the wide part [Fig. 5(c)].

2.3.2. Polarization drift measurements in sT-DCF

The experimental setup for measuring polarization drift in a spun fiber is similar to that used in the experiments with the other two types of fibers [Fig. 1(b)]. The results are shown in Fig. 6. In

Optics EXPRESS

line with the experimental results for the active spun fiber, an increase of launched pump power up to 23 W is accompanied by a rise in the temperature of the fiber surface by ~2°C. The changes of SOP in the amplifier with an active spun fiber were much lower. The change of azimuth is almost by an order of magnitude better for the spun active fiber than for the PANDA: 1.2° vs 8.9°. The change of ellipticity is 12 times better: 0.6° vs. 7.2°. The DOP and PER exhibited only minor degradation of 3.6% and 2 dB, respectively.

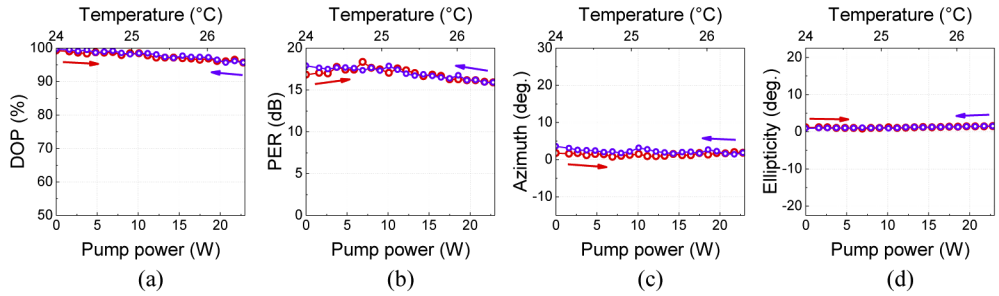

Fig. 6. (a) DOP, (b) PER, (c) azimuth, and (d) ellipticity vs pump power and fiber temperature for an active sT-DCF.

2.3.3. Measurements of internal birefringence at sT-DCF

Characterization of ultra-low birefringence fibers is a challenging task and it is even more difficult for short fibers. The vast majority of methods described in the literature require long fibers in order to detect ultra-low birefringence values. The approach we use in this work is based on Jones method [21,22] for determining the transfer matrix of a spun T-DCF and the assumption that linear birefringence is caused only by fiber bending. This is a realistic assumption since the linear birefringence associated with fiber asymmetry is averaged over all directions by rotating the preform during the fiber drawing. The Jones matrix describes the relation between the circular and linear components of birefringence, and the latter can be found if the fiber bending radius is known [23]. Thus, calculations yield 1.45×10^{-8} and 2.52×10^{-9} for circular and linear birefringence, respectively. More details can be found in Supplement 1.

3. Picosecond MOPA with sT-DCF

To investigate the amplification properties of an active sT-DCF, we built a so-called master oscillator power amplifier (MOPA) system (Fig. 7). We used a similar 3 m sT-DCF. The Yb-doped sT-DCF was tested as a high-power amplifier seeded at 1040 nm. A commercially available gain-switched diode was used as a source with a central wavelength of 1040 nm. It generated 50 ps pulses with a repetition rate of 20 MHz, a linewidth of 0.1 nm, and an average output power of 300 μW. We also included a pre-amplifier to reach the sufficient average power level of 20 mW typically used in our experiments. The output of each seed laser was spliced with a high-power isolator to prevent damage to the seed laser.

A counter-pumping scheme was used in this experiment. The signal was coupled into the narrow side of the sT-DCF via splicing while pumping from the wide side was performed using a free-space dichroic filter and focusing lens. A wavelength-stabilized laser diode with a nominal power of 100 W was used to pump from the wide side. The sT-DCF was placed into the metal grooves of a massive plate with water cooling to provide effective heat dissipation. Since the wide side of the tapered fiber is the hottest part of the fiber, we covered the first 30 cm with thermal paste to avoid damage. For the amplification of the 1040 nm seed signal, we pumped 100 W power and reached 50 W of the output power with a corresponding gain of 34 dB [Fig. 8(a)]. The output spectra for the amplified signal are shown in Fig. 8(b).

Optics EXPRESS

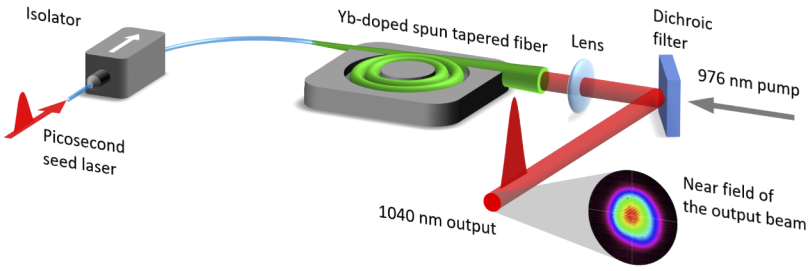

Fig. 7. Scheme of MOPA system based on an active sT-DCF.

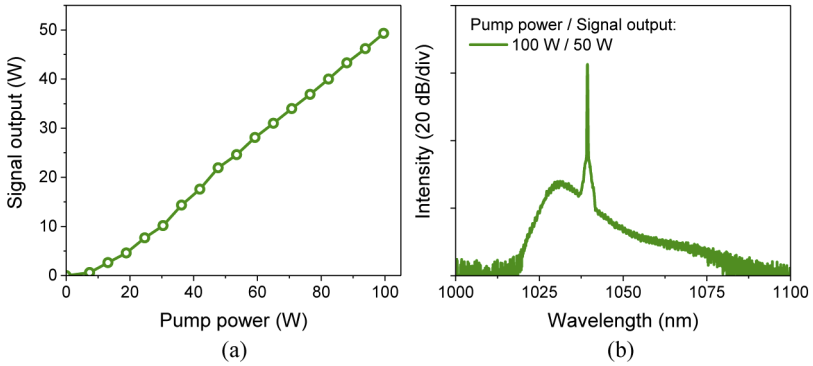

Fig. 8. Output characteristics of a MOPA system based on an active sT-DCF. (a) spectrum of the amplified 1040 nm signal at maximum output power; (b) signal output vs pump power.

The output beam of the sT-DCF-based amplifier had a near diffraction-limited fundamental mode with $M_x^2 = 1.18$ and $M_y^2 = 1.10$ (Fig. 7). We estimated a mode field diameter at the level of 13.5%. For the sT-DCF with the core diameter of 35 μm, the MFD was 26 μm and it occupied 74% of the core.

The SOP drift in the MOPA system is shown in Fig. 9. The DOP gradually decreased from 99% to 94% along with an increase in the pump power. The PER was higher than 15 dB up to 60 W pump power and then it gradually decreased down to 10 dB. This was due to the fact that at a pump power of 60 W the sT-DCF began to overheat, the temperature of the wide end increased, and at maximum power of 100 W it reached 79°C. Considering that most of the fiber had a temperature of about 24°C, the huge temperature gradient created by the pumping caused

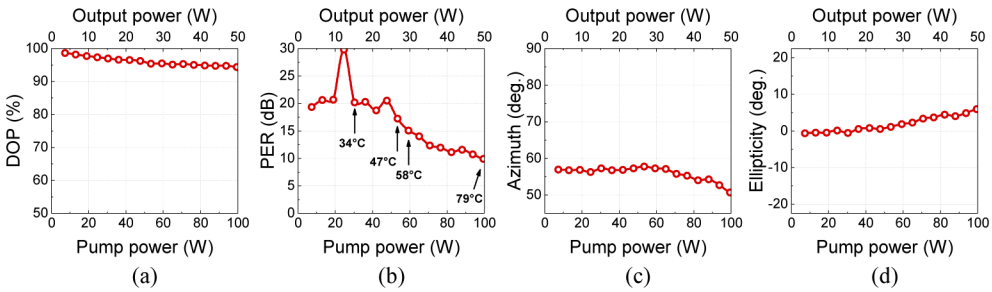

Fig. 9. SOP drift in MOPA system based on the active sT-DCF. The arrows indicate the temperature of the sT-DCF wide end.

Optics EXPRESS

the SOP drift. Thus, the optimal pumping range for the sT-DCF with this particular geometry was 0-60 W. Having a larger temperature gradient (pumping range 0-60 W), the sT-DCF exhibits less SOP drift than the PANDA-type tapered fiber. More thorough cooling and optimized fiber geometry should improve the current result and increase the pump power range where the SOP is stable.

4. Discussion

An ideal optical fiber guides all the polarization modes equally and they are degenerated by the propagation constant. However, any external perturbation of a fiber or its internal inhomogeneity lift the degeneracy of the polarization modes by the propagation constant and the fiber becomes more like a uniaxial crystal. The perturbations which lift the degeneracy of the polarization modes in the fiber can be divided into internal and external ones. External perturbations are usually macro-effects that change the shape of the fiber (different kinds of bends), the transversal compressions, twisting and the magnetic or electric fields [6].

Internal perturbations can be further divided into induced and random perturbations. Induced internal perturbations are originated by an asymmetrical (elliptical) core, built-in mechanical stresses induced by borosilicate elements in the cladding (PANDA or bow-tie type), or an asymmetrical clad [6]. Random internal stresses are determined by variations of the optical properties of the core material and are usually caused by features of doping technology or by the manufacturing of the active optical fibers. The production of an active optical fiber, including doping by rare-earth ions and drawing the fiber, is accompanied by the formation of strong local mechanical stresses in the core. These are inhomogeneous both in cross-section [24–27] and along the fiber length [12,28]. Recently, it was experimentally demonstrated [12,24] that the active core heating due to a quantum defect is strongly inhomogeneous along the fiber length, and apparently, reflects the longitudinal inhomogeneity of Yb^{3+} ions doping (clustering). It is well known that even doping by Al or P leads to the appearance of essential mechanical stresses in the core of the preforms/fibers [24–26], which in turn causes a strong local birefringence. In [24], it was demonstrated that doping by Yb^{3+} ions leads to significant mechanical stresses and local changes in the refractive index up to 10^{-4}. Thus, the optical properties of an active optical fiber are substantially longitudinally inhomogeneous.

In this work, we experimentally investigated the evolution of the SOP (DOP and shape of the polarization ellipse) of light after propagation in active clad pumped T-DCF. The SOP drift was a result of the fiber heating due to pump absorption. In the experiments, we used a pump source powerful enough to cause noticeable heating of the fiber up to several degrees Celsius (976 nm, 23 W) in the setup, without special cooling. The temperature was measured on the surface of the T-DCF at a distance of 5 cm from the pump launching point (the wide end).

We carried out a comparative study of the SOP evolution for three types of active T-DCF:

- regular non-PM T-DCF, similar to those used earlier in [29];
- PANDA-type T-DCF with a strong internal birefringence;
- spun T-DCF with low intrinsic birefringence; presented for the first time in this work.

Each of these fibers has both internally and externally induced components of birefringence of differing magnitude and in different combinations. The common externally induced birefringence for all three fibers is a linear birefringence caused by their identical coiling with a diameter of 35 cm.

4.1. Active non-PM T-DCF

The strong depolarization of narrow-band emission (20 pm) at the non-PM (isotropic) active T-DCF can be qualitatively explained by using the model of isotropic fiber proposed earlier in

Optics EXPRESS

[30]. A regular isotropic optical fiber was considered as a sequence of randomly oriented phase plates, relative to each other, with different (also random) retardance at each phase plate [30].

T-DCF can also be represented as a sequence of cylindrical single-mode fibers with a smoothly increasing core diameter, each of which is equivalent to a phase plate (Fig. 10) [31]. Although the concentration of dopants is the same everywhere, the number of ions in the neighboring parts of the T-DCF is different due to the different core volumes. Since rare-earth dopants induce a strong internal stress [24], adjacent sections of a tapered fiber have different birefringence values, and the birefringence axes of the next elementary sections are oriented randomly with respect to each other. The optical scheme shown in Fig. 10 qualitatively represents a multi-stage Lyot depolarizer with random parameters [32]. The parameters of this depolarizer, such as the orientation of the axes and the retardance of each elementary local phase plate depend on the fiber's internal temperature. This, in turn, is distributed non-uniformly in the longitudinal direction [12]. Accordingly, the depolarizing properties of such a natural depolarizer are also determined by the level of absorbed pump power. Thus, in the polarization sense, an active optical fiber is a complicated optical device that can simultaneously possess both depolarizing and phase plate properties.

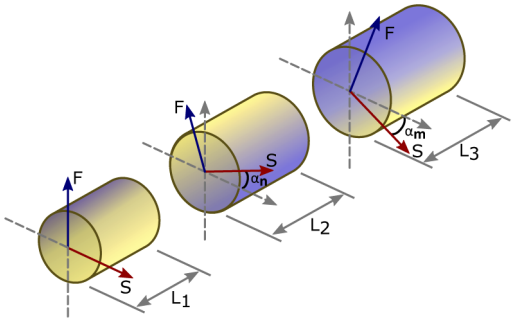

Fig. 10. The equivalent scheme of the isotropic active tapered fiber.

An active non-PM T-DCF is equivalent to a random Lyot depolarizer and, at the same time, it is a linear phase plate with its integral birefringence mainly determined by the fiber bending. Therefore, when light propagates and amplifies in non-PM T-DCF, a partial depolarization occurs. The SOP of the polarized part of the light is changed as it occurs during propagation in the linear phase plate.

Experiments with a non-PM T-DCF demonstrate a good match with the proposed model. The propagation and amplification throughout a 3.2 m non-PM T-DCF lead to a significant depolarization of a narrow-band seed laser emission [Fig. 2(a)]. An initially 100% linearly polarized light with only 20 pm FWHM becomes partially depolarized with 75% DOP even in the absence of pumping. Increasing the launched pump power up to 23 W leads to rapid degradation of the DOP down to 55%. When the pump power decreases, the DOP recovers its original state in a reversible manner without any hysteresis. Thus, during propagation (amplification) through a regular T-DCF, a significant depolarization of light occurs that further increases in line with an increase in the launched pump power. A 40% reversible depolarization was measured at 23 W pump power, which causes the fiber to be heated by only 6°C. Due to the heating of the fiber, the clad pumping leads to a deeper and spatially non-uniform modulation of the longitudinal refractive index profile [12]. As a result, the internal built-in Lyot depolarizer becomes more pronounced, which, in turn, leads to degradation of the DOP.

Coiling a fiber causes a bending-induced birefringence, which also varies with clad pumping. This variation leads to a change in retardance and, ultimately, to a change of SOP [azimuth and ellipticity Eq. (4)]. In our experiments, we investigated changes of the azimuth and ellipticity

Optics EXPRESS

with respect to the launched pump power [Figs. 2(c) and (d)]. At the maximum pump level, the azimuth and ellipticity changed by about 6 degrees.

The fact that the degree of depolarization of a single-mode laser/amplifier can be effectively controlled by varying the pump power opens up the prospect of creating powerful light sources with controlled DOP and high spectral brightness. Such optical sources are potentially in demand for metrology and sensor applications [33]. The significant depolarization in a non-PM T-DCF (25-50%) also explains the lower SOP sensitivity in this fiber. Indeed, the SOP of the non-polarized part of the light is insensitive to any retardance changes; as a result, the increase of the non-polarized fraction of the output power looks like a lower sensitivity of the SOP with respect to the launched pump power. In fact, the fraction of polarized light that responds to the retardance changes only decreases with increasing pump power.

4.2. Active PM T-DCF

A PM T-DCF exhibits internal birefringence induced by the stress-rods which is much larger than the bend-induced birefringence, the birefringence caused by rare-earth ions doping or mechanical stress formed during the drawing process [24–28]. As a result, a PM T-DCF is more like a linear phase plate than a random Lyot depolarizer (Fig. 10). This conclusion is confirmed experimentally by the retention of almost 100% DOP while increasing the launched pump power [Fig. 4(a)]. The SOP sensitivity (ellipticity, azimuth and PER) to the launched pump power for a PM T-DCF is significantly higher than it is for a non-PM T-DCF. The PER varied within an 11.5 dB range for 23 W launched pump power [Fig. 4(b)], while the azimuth and ellipticity changed by 8.9° and 7.2°, respectively [Figs. 4(c) and 4(d)].

Theoretically, if only the sole eigenstate is precisely excited, the SOP should be stable after passing the phase plate. In our experiments, we aimed to excite the sole linear eigenstate. However, the ellipticity and azimuth changed periodically when pump power increased (Fig. 4) which was a good match with the theory see Eq. (4), this study and Eqs. (3.29-3.30) [14]. Indeed, the ellipticity and azimuth are in quadrature with respect to the retardance. Thus, upon pumping into the cladding, a change occurs in the retardance, and, as follows from Eqs. (2) and 3, the retardance changes are due to a change of the birefringence.

When launched into the fiber, the pump intensity decreases along the length of the fiber due to absorption and this leads to a temperature gradient. At the same time, the absolute temperature also inevitably increases. In PM fibers, birefringence changes with temperature mainly because the stress rods and cladding are made of materials that have different thermal expansion coefficients. As soon as the temperature changes, the internal stress in the fiber also changes, and this leads to a variation in the birefringence. This effect of changes in the SOP in line with increasing pump power is not new, and many other researchers have observed it. Recently, some publications have reported deterioration of the PER by 7 dB at 300 W of launched pump power in a system with 25/250 μm birefringent LMA fiber. This occurred despite the application of temperature stabilization measures for the active fiber [34].

Light depolarization, caused by the doping-induced internal stresses, is the main obstacle to the development of an active fiber suitable for the efficient amplification of polarized light. In active PM T-DCF and sT-DCF, two opposing strategies are employed to overcome the depolarization problem. In a PM T-DCF, a very large internal birefringence (usually linear) is induced, which is much larger than the random birefringence caused by doping. As a result, the PM T-DCF is equivalent to a phase plate with a large intrinsic birefringence.

4.3. Active spun T-DCF

The drawing process of sT-DCF is accompanied by fast preform rotation (600 rev/min) which leads to an efficient averaging of local inhomogeneities in an active core. These are associated with Yb^{3+} doping [24] and may also arise during the fiber drawing (stresses and geometric

Optics EXPRESS

defects) [28]. The natural Lyot depolarizer disappears due to a large number of twists and the averaging of the frozen inhomogeneities. Basically, an sT-DCF is also a waveplate, but one with its own very small (10^{-8}) elliptical birefringence. This elliptical birefringence of the sT-DCF is a combination of circular and linear birefringence. Circular birefringence (optical activity) is determined by residual frozen mechanical twist stresses, which are the consequence of the preform rotation. The linear part of the birefringence is defined by the fiber bending caused by the coiling, which is unavoidable (35 cm diameter). This linear birefringence determines the azimuth drift [Fig. 6(c)]. Our experiment showed 99% DOP at the output of the sT-DCF, which deteriorated slightly (by 3.6%) with a 23 W pumping (Fig. 6). Accordingly, sT-DCF does not depolarize the amplified light. At the same time, the change of SOP in the active sT-DCF is much smaller than it is with both isotropic and PANDA-type T-DCFs (Fig. 6 and Table S2 in Supplement 1). The reason for this is the low intrinsic birefringence (1.45×10^{-8}). Thus, the change in ellipticity after propagation through sT-DCF at 23 W of the pumping power is only 0.6° [Fig. 6(d)].

Another important advantage of spun double-clad fiber is the slightly higher clad pump absorption (0.2-0.3 dB/m) compared to the same fiber which has not been rotated during the drawing process. Indeed, the rotation of the preliminary shaped preform always leads to better mixing of the cladding modes [35] and to a slightly better cladding absorption, which also occurs in this case. Potentially, sT-DCF can be used as a gain medium for a circularly polarized seed source to create an efficient pulsed amplifier with a low ASE level that is free of polarization hole burning (PHB) [36]. sT-DCF appears to be an excellent candidate for an orbital angular momentum OAM beam amplifier. On the one hand, sT-DCF does not depolarize amplified radiation, as happens in active non-PM optical fibers. On the other hand, having a circular polarization as an eigenstate, it does not suffer from PHB and amplifies any polarization equally. In the future, we are planning to continue research in this direction.

5. Conclusion

The present work addresses the problem of polarization state drift in active double-clad optical fibers, which occurs under clad pumping. A comparative experimental study of isotropic and anisotropic T-DCFs revealed that the SOP drift was associated with a quantum defect. We found out that the light propagation in active isotropic T-DCFs is accompanied by strong depolarization of light; up to 55% at 23 W pumping. This increases with the pumping launching into the fiber. We have proposed a model that qualitatively describes this effect. The DOP in a PANDA-type T-DCF was insensitive to the pumping. However, the PER varied periodically within the 8.9-20.4 dB range.

In this work, we proposed a solution to the problem of SOP drift in active fibers, namely, the use of an active fiber with low intrinsic birefringence. This was the first time, that an active tapered fiber with a low intrinsic birefringence (spun fiber) of 1.45×10^{-8} has been manufactured. The fiber had an MFD of 26 μm and delivered a perfect output beam with M^2 = 1.1. The measured sensitivity of the polarization state in an active spun fiber was more than an order of magnitude lower than in a comparable anisotropic fiber. The manufactured spun T-DCF had intrinsic polarization states close to circularity and maintained the propagation of both linearly and circularly polarized light with a DOP of 98%. The fiber exhibited very slight hysteresis of the polarization state (0.6% for ellipticity and 2.3% for azimuth) at 23 W launched pump power. This is caused by the inertia of the thermal processes. The amplification properties of a novel sT-DCF were investigated in a picosecond MOPA system which delivered an output power of 50 W (34 dB gain, 50 ps, 47 kW peak power, and 2.5 μJ pulse energy).

Funding. Ministry of Science and Higher Education of the Russian Federation (0030-2019-0015); Russian Science Foundation (19-79-00371); Academy of Finland (320165).

Disclosures. J.R.: Ampliconyx Ltd. (E), R.G.: Ampliconyx Ltd. (I), Y.C. (P), V.F.: Ampliconyx Ltd. (E,P,I)

Optics EXPRESS

Supplemental document. See Supplement 1 for supporting content.

References

1. D. A. V. Kliner, J. P. Koplow, L. Goldberg, A. L. G. Carter, and J. A. Digweed, "Polarization-maintaining amplifier employing double-clad bow-tie fiber," Opt. Lett. **26**(4), 184–186 (2001).
2. O. Schmidt, J. Rothhardt, T. Eidam, F. Röser, J. Limpert, A. Tünnermann, K. Hansen, C. Jakobsen, and J. Broeng, "Single-polarization large-mode-area Yb-doped photonic crystal fiber," in *Conference on Lasers and Electro-Optics/Quantum Electronics and Laser Science Conference and Photonic Applications Systems Technologies* (Optical Society of America, 2008), p. CMB2.
3. A. Fedotov, T. Noronen, R. Gumenyuk, V. Ustimchik, Y. Chamorovskii, K. Golant, M. Odnoblyudov, J. Rissanen, T. Niemi, and V. Filippov, "Ultra-large core birefringent Yb-doped tapered double clad fiber for high power amplifiers," Opt. Express **26**(6), 6581–6592 (2018).
4. A. Ourmazd, M. P. Varnham, R. D. Birch, and D. N. Payne, "Thermal properties of highly birefringent optical fibers and preforms," Appl. Opt. **22**(15), 2374–2379 (1983).
5. S. C. Rashleigh and M. J. Marrone, "Temperature dependence of stress birefringence in an elliptically clad fiber," Opt. Lett. **8**(2), 127–129 (1983).
6. S. Rashleigh, "Origins and control of polarization effects in single-mode fibers," J. Lightwave Technol. **1**(2), 312–331 (1983).
7. I. Kaminow, "Polarization in optical fibers," IEEE J. Quantum Electron. **17**(1), 15–22 (1981).
8. D. C. Brown and H. J. Hoffman, "Thermal, stress, and thermo-optic effects in high average power double-clad silica fiber lasers," IEEE J. Quantum Electron. **37**(2), 207–217 (2001).
9. Wang Yong, Xu Chang-Qing, and Po Hong, "Thermal effects in kilowatt fiber lasers," IEEE Photonics Technol. Lett. **16**(1), 63–65 (2004).
10. V. V. Gainov, R. I. Shaidullin, and O. A. Ryabushkin, "Steady-state heating of active fibres under optical pumping," Quantum Electron. **41**(7), 637–643 (2011).
11. M. K. Davis, M. J. F. Digonnet, and R. H. Pantell, "Thermal effects in doped fibers," J. Lightwave Technol. **16**(6), 1013–1023 (1998).
12. Z. Lou, B. Yang, K. Han, X. Wang, H. Zhang, X. Xi, and Z. Liu, "Real-time in-situ distributed fiber core temperature measurement in hundred-watt fiber laser oscillator pumped by 915/976 nm LD sources," Sci. Rep. **10**(1), 9006 (2020).
13. G. B. Hocker, "Fiber-optic sensing of pressure and temperature," Appl. Opt. **18**(9), 1445–1448 (1979).
14. A. Yariv and P. Yeh, *Optical waves in crystals: propagation and control of laser radiation*, Wiley classics library (John Wiley and Sons, Hoboken, N.J, 2003).
15. S. R. Norman, D. N. Payne, M. J. Adams, and A. M. Smith, "Fabrication of single-mode fibres exhibiting extremely low polarisation birefringence," Electron. Lett. **15**(11), 309–311 (1979).
16. H. Schneider, H. Harms, A. Papp, and H. Aulich, "Low-birefringence single-mode optical fibers: preparation and polarization characteristics," Appl. Opt. **17**(19), 3035–3037 (1978).
17. A. J. Barlow, J. J. Ramskov-Hansen, and D. N. Payne, "Birefringence and polarization mode-dispersion in spun single-mode fibers," Appl. Opt. **20**(17), 2962–2968 (1981).
18. D. N. Payne, A. J. Barlow, and J. J. Ramskov Hansen, "Development of low- and high-birefringence optical fibers," IEEE Trans. Microwave Theory Tech. **30**(4), 323–334 (1982).
19. Y. Chamorovskiy, N. Starostin, M. Ryabko, A. Sazonov, S. Morshnev, V. Gubin, I. Vorob'ev, and S. Nikitov, "Miniature microstructured fiber coil with high magneto-optical sensitivity," Opt. Commun. **282**(23), 4618–4621 (2009).
20. J. Rissanen, A. Fedotov, T. Noronen, R. Gumenyuk, Y. Chamorovskiy, A. Kolosovskii, V. Voloshin, I. Vorobev, M. Odnoblyudov, and V. Filippov, "Large-mode-area double clad ytterbium-doped tapered fiber with circular birefringence," in *Fiber Lasers XVI: Technology and Systems*, vol. 10897 A. L. Carter and L. Dong, eds., International Society for Optics and Photonics (SPIE, 2019), pp. 342–349.
21. R. C. Jones, "A new calculus for the treatment of optical systems. VI. Experimental determination of the matrix*," J. Opt. Soc. Am. **37**(2), 110–112 (1947).
22. Y. Wang, C.-Q. Xu, and V. Izraelian, "Characterization of spun fibers with millimeter spin periods," Opt. Express **13**(10), 3841–3851 (2005).
23. R. Ulrich, S. C. Rashleigh, and W. Eickhoff, "Bending-induced birefringence in single-mode fibers," Opt. Lett. **5**(6), 273–275 (1980).
24. F. Just, H.-R. Müller, S. Unger, J. Kirchhof, V. Reichel, and H. Bartelt, "Ytterbium-doping related stresses in preforms for high-power fiber lasers," J. Lightwave Technol. **27**(12), 2111–2116 (2009).
25. G. W. Scherer, "Stress-induced index profile distortion in optical waveguides," Appl. Opt. **19**(12), 2000–2006 (1980).
26. O. E. Shushpanov, A. N. Tuzov, I. V. Alexsandrov, S. P. Vikulov, M. E. Zhabotinskii, V. V. Romanovtzev, and S. J. Feld, "An automated system for measurement of mechanical stresses in optical fiber preforms with polarization-optical method," Radiotechnika 67–72 (1988).
27. M. R. Hutsel, R. Ingle, and T. K. Gaylord, "Accurate cross-sectional stress profiling of optical fibers," Appl. Opt. **48**(26), 4985–4995 (2009).
28. F. Just, R. Spittel, J. Bierlich, S. Grimm, M. Jäger, and H. Bartelt, "The influence of the fiber drawing process on intrinsic stress and the resulting birefringence optimization of pm fibers," Opt. Mater. **42**, 345–350 (2015).

Optics EXPRESS

29. V. Filippov, Y. Chamorovskii, J. Kerttula, K. Golant, M. Pessa, and O. G. Okhotnikov, "Double clad tapered fiber for high power applications," Opt. Express **16**(3), 1929–1944 (2008).
30. T. Chartier, A. Hideur, C. Özkul, F. Sanchez, and G. M. Stéphan, "Measurement of the elliptical birefringence of single-mode optical fibers," Appl. Opt. **40**(30), 5343–5353 (2001).
31. V. Filippov, J. Kerttula, Y. Chamorovskii, K. Golant, and O. G. Okhotnikov, "Highly efficient 750 W tapered double-clad ytterbium fiber laser," Opt. Express **18**(12), 12499–12512 (2010).
32. W. Burns, "Degree of polarization in the lyot depolarizer," J. Lightwave Technol. **1**(3), 475–479 (1983).
33. H. C. Lefèvre, "The fiber-optic gyroscope: Challenges to become the ultimate rotation-sensing technology," Opt. Fiber Technol. **19**(6), 828–832 (2013).
34. F. Wellmann, M. Steinke, F. Meylahn, N. Bode, B. Willke, L. Overmeyer, P. Weßels, J. Neumann, and D. Kracht, "Low-noise, single-frequency 200 W fiber amplifier," in *Fiber Lasers XVII: Technology and Systems*, vol. 11260 L. Dong, ed., International Society for Optics and Photonics (SPIE, 2020), pp. 125–131.
35. P. Koška, P. Peterka, J. Aubrecht, O. Podrazký, F. Todorov, M. Becker, Y. Baravets, P. Honzátko, and I. Kašík, "Enhanced pump absorption efficiency in coiled and twisted double-clad thulium-doped fibers," Opt. Express **24**(1), 102–107 (2016).
36. V. J. Mazurczyk, R. H. Stolen, J.-S. Wang, and C. D. Poole, "Observation of polarization hole burning in Er-doped fiber for circular polarization of the saturating signal," in *Optical Fiber Communications Conference* (Optical Society of America, 1995), p. TuJ7.